



Size-dependent distribution and inhalation exposure characteristics of particle-bound chlorinated paraffins in indoor air in Guangzhou, China

Wei Zhou^a, Mingjie Shen^a, James C.W. Lam^b, Mingshan Zhu^a, Liangying Liu^a, Hui Chen^a, Bibai Du^a, Lixi Zeng^{a,*}, Eddy Y. Zeng^a

^a School of Environment and Guangdong Key Laboratory of Environmental Pollution and Health, Jinan University, Guangzhou 510632, China

^b Department of Science and Environmental Studies, The Education University of Hong Kong, Hong Kong SAR, China



ARTICLE INFO

Handling editor: Xavier Querol

ABSTRACT

Chlorinated paraffins (CPs) are now attracting special concerns worldwide as one type of new persistent toxic substances as classified by the Stockholm Convention. CPs are extensively applied in household goods and indoor decoration materials, but information on their occurrence and exposure risk in such environments is still very scarce. In this study, the current concentrations, particle size distributions, and inhalation exposure characteristics and risk of CPs were investigated in regard to indoor air particulate matter. Both short chain (SCCPs) and medium chain CPs (MCCPs) were determined in all size-fractionated particle samples with a range of 6.20–17.8 and 5.98–40.5 ng m⁻³, respectively. MCCPs were more abundant than SCCPs. Size distributions revealed that individual homologs, SCCPs, and MCCPs exhibited a similar unimodal distribution peaking in the fine particles with a diameter of 0.56–1.0 μm. The relative abundance of longer-chain or more heavily chlorinated homologs tend to gradually increase with particle size shift from coarse to fine mode. Vapor pressure may be a critical factor governing the size-dependent distribution of CPs. Deposition of particulate CPs in the human respiratory tract is also size-dependent. The contributions of fine particles to the regional depositions of CPs in the human respiratory tract increase with increasing carbon chain length or chlorine content. Based on the size-dependent distributions of CPs, inhalation exposure assessment from the ICRP model indicated no significant health risk due to CPs in current indoor environments.

1. Introduction

Chlorinated paraffins (CPs) are complex industrial chemicals consisting of thousands of homologs and isomers with chlorine contents of 30–70%. The commercial CPs are generally classified based on the carbon chain length into short chain CPs (SCCPs, C₁₀–C₁₃), medium chain CPs (MCCPs, C₁₄–C₁₇), and long chain CPs (LCCPs, C₁₈–C₃₀). They are widely applied as plasticizers in polyvinyl chloride (PVC) and flame retardants in many commercial products (UNEP, 2016). Production and use amounts of CPs exceeded 1000 kt in 2013, and thus CPs are identified as having the highest production volume among current industrial chemicals (Glüge et al., 2018). China is still the globally largest producer, consumer and exporter of CPs at present, and the emission alone of SCCPs in China could be up to 2.56 kt in 2016 (Xu et al., 2014). In the last few years, CP research has focused mainly on SCCPs relative to MCCPs and LCCPs because of their higher environmental persistence, long-distance migration abilities, bioaccumulation and biomagnification, and greater toxicological and potential endocrine disruption

effects (UNEP, 2016; van Mourik et al., 2016). SCCPs have been shown to affect the thyroid, liver and kidneys by causing hepatic enzyme induction and thyroid hyperactivity, which in the long-term can result in carcinogenicity in these organs (UNEP, 2016). Therefore, SCCPs are suspected to cause cancer in humans and disrupt endocrine function. In view of these severe adverse health effects, SCCPs have been added to the list of Persistent Organic Pollutants (POPs) by the Stockholm Convention as a kind of new POPs in May 2017 (UNEP, 2017). Compared to SCCPs, MCCPs have been less well studied (Glüge et al., 2018). The available data suggest that MCCPs are more bioaccumulative than SCCPs (Zeng et al., 2017a), and present similar ecological risks as SCCPs (Kobeticova and Cerny, 2018). The production amounts of MCCPs on a global scale are estimated to be much higher than those of SCCPs (Glüge et al., 2018; Glüge et al., 2016), and especially MCCPs are often frequently detected at higher levels in various matrices than SCCPs (Gallistl et al., 2018). With the phasing out and banning of SCCPs, MCCPs are suggested to be a suitable and a preferred alternative to SCCPs (Kobeticova and Cerny, 2018). Therefore, MCCPs are also of

* Corresponding author.

E-mail address: lxzeng@jnu.edu.cn (L. Zeng).

<https://doi.org/10.1016/j.envint.2018.10.004>

Received 11 July 2018; Received in revised form 1 October 2018; Accepted 2 October 2018

Available online 11 October 2018

0160-4120/ © 2018 Elsevier Ltd. All rights reserved.

currently great concern in regard to the environment (Glüge et al., 2018; Wang et al., 2017).

Widespread use of CP-added products in houses, such as PVC flooring, increases the opportunities for fugitive emissions of CPs to enter the indoor environment including dust, air, and suspended particles (Zhan et al., 2017). Indoor concentrations of CPs have been sporadically reported in Europe and China (Friden et al., 2011; Gao et al., 2018; Hilger et al., 2013; Zhu et al., 2017), and in general, they are found to be higher than in outdoor settings although particulate matter (PM) mass concentrations in indoor environments are relatively lower (Huang et al., 2017). Thus, indoor CPs in highly urbanized areas can pose a higher health risk than outdoor CPs. This is because urban residents, especially the elderly and young children, tend to spend more time indoors. Secondly, CPs associated with indoor PM are expected to be more persistent due to their slow oxidative degradation under suppressed levels of hydroxyl radicals (Li et al., 2014; Zhang et al., 2012). In addition, depositing particles can form indoor dust. Thus, inhalation is believed to be an important exposure pathway of CPs to humans in indoor environments.

Inhalation exposure is the most difficult to regulate and thus can be used as an excellent indicator of human health hazards among the four main exposure pathways, i.e., inhalation, food intake, dermal adsorption, and dust ingestion (Luo et al., 2014a). Previous studies indicated that the size distribution of particulate contaminants is a key factor controlling their behavior and fate in the atmosphere, and the contributions of particle-bound toxic chemicals to inhalation exposure risk is strongly particle size-dependent (Luo et al., 2014a; Luo et al., 2016; Yang et al., 2014). For example, particles with different sizes can accumulate in different regions with size-specific deposition efficiencies in the human respiratory system. In general, smaller size particles can carry more contaminants and enter into the deeper respiratory system, and pose a higher risk than coarse particles (Zhang et al., 2012). Although a few published concentrations of indoor particulate CPs in urban regions can be used to evaluate inhalation exposure levels, not all of these CPs can deposit in the respiratory tract or go deep into the lungs. Thus, the size distribution of particle-bound CPs must be considered when inhalation exposure is evaluated, which is crucial for accurate evaluation of the risk of exposure to inhaled CPs. Among the published studies, only one study focused on the levels and compositions of CPs in airborne PM₁₀/PM_{2.5}/PM_{1.0} (Huang et al., 2017). To date, no size-dependent distribution of particle-bound CPs has been systematically investigated, and also no size effect has been taken into account in the assessment of inhalation exposure to particle-bound CPs in indoor air.

To fill this knowledge gap, we carried out the first systematic study on the particle size distribution of CP homologs in indoor air. Suspended particles with different diameters were collected from 10 offices and 5 residential homes at urban sites in Guangzhou, and were simultaneously analyzed for SCCPs and MCCPs on the particles. The current study therefore aimed to (1) reveal the current level and detailed size distribution of atmospheric particle-bound CPs; (2) explore the potential mechanism for the size distribution of CPs in size-fractionated particles; (3) evaluate the size-dependent respiratory deposition of particle-bound CPs; and (4) characterize the inhalation exposure to particulate CPs based on their size distribution in indoor air. The results of this study are expected to provide a deeper cognition of the behavior, fate and human health risk of CPs in indoor environments.

2. Materials and method

2.1. Field sampling

Size-segregated PM samples were collected in 10 office rooms and 5 residential homes during October to December 2017 in the city center locations of Guangzhou (23°7' N and 113°20' E), China. Ten offices were selected in separate areas located in three office buildings of the

city center. These offices were far away from industrial activity and approximately 100 m away from a main road, which were furnished with common desks, filing cabinets and office electronic products including computers and printers but differed in the type and number of these items. Five residential houses were randomly selected in two populated areas which were about 500 m away from a main road. These houses were built in the 2000s and have not been redecorated in recent years. They were equipped with essential furniture and household electrical appliances with no upgrading or replacement in the last few years. The selected 15 sampling sites can represent the typical urban offices and homes in the megacities of South China according to our survey. The sampling was conducted on a desk near the central area of the room and placed at 1 m above the ground by an 11-stage Micro-Orifice Uniform Deposit Impactor (MOUDI) (MSP Corporation, Shoreview, MN). All doors were closed in the rooms with the windows slightly open to simulate common indoor environments. The weather was sunny with the temperature ranging from 16 to 25 °C and the humidity ranging from 35 to 50% during the sampling time. Each size segregated PM sample was collected on prebaked glass microfiber filters (GFF, 47 mm i.d., Whatman) at a constant flow rate of 30 L min⁻¹. Particle samples were separated by cutoff aerodynamic diameters (D_p) into 11 fractions as > 18, 10–18, 5.6–10, 3.2–5.6, 1.8–3.2, 1.0–1.8, 0.56–1.0, 0.32–0.56, 0.18–0.32, 0.10–0.18, and 0.056–0.10 μm, respectively. Size segregated particles were subdivided into coarse ($D_p > 1.8 \mu\text{m}$), fine ($0.10 < D_p < 1.8 \mu\text{m}$), and ultrafine ($D_p < 0.10 \mu\text{m}$). In order to collect sufficient particle mass and minimize the interday variations, each sampling was conducted for a continuous 48 h. The total air volume for each sampled room was 86.4 m³. Overall, a total of 165 field particle samples (15 suits of samples containing 11 size-segregated fractions) were collected. Field blanks were prepared during the period of sampling by mounting GFFs to the MOUDI sampler. After sampling, the GFF filters were placed into clean glass boxes, wrapped in aluminum foil and then stored at -20 °C.

2.2. Sample preparation, instrumental analysis, identification and quantification

Sample preparation was performed according to the previously developed procedures with minor modifications (Zeng et al., 2012, 2013; Zeng et al., 2017b). Detailed information is presented in the Supplementary Information (SI). SCCPs and MCCPs were simultaneously analyzed by high-resolution gas chromatography equipped with a low-resolution mass spectrometer (Agilent 7890B-7000D, USA) using an electron capture negative ion (ECNI) mode based on our previously developed method (Zeng et al., 2011; Zeng et al., 2015; Zeng et al., 2017b). Detailed information with regard to the instrumental analysis, identification and quantification is also given in the SI.

2.3. Quality assurance and quality control (QA/QC)

All glassware was carefully solvent-rinsed and then heated for 5 h at 450 °C prior to use to eliminate potential background contamination. Every batch consisting of five samples was followed by a procedural blank. SCCPs or MCCPs in the procedure blanks and field blanks were below the limits of detection, and thus the reported concentrations of SCCPs or MCCPs were not blank-corrected. The recoveries of SCCP standards (chlorine content: 51.5%, 55.5% and 63.0%) and MCCP standards (chlorine content: 42.0%, 52.0% and 57.0%) in spiked samples were 72–102% and 75–103%, respectively, and the relative standard deviations (RSDs) were < 10% ($n = 7$). The surrogate recoveries of ¹³C₁₀-1,5,5,6,6,10-hexachlorodecane (Fig. S1) in all of the samples were between 70% and 105%, and the final concentrations were corrected by the surrogate. The method detection limits (MDLs) were estimated to be 0.4 ng m⁻³ for the total SCCPs (ΣSCCPs) and 0.6 ng m⁻³ for total MCCPs (ΣMCCPs) based on three times the standard deviation of blank values.

2.4. Calculation of geometric mean diameter (GMD) and geometric standard deviation (GSD)

To explore the characteristics and potential mechanism of particle size distribution of the individual CP homologs, the GMD and GSD were calculated by the following equations (Hinds, 1999; Lao et al., 2018; Luo et al., 2015):

$$\log \text{GMD} = \frac{\sum C_i \log D_{p,i}}{\sum C_i}$$

$$(\log \text{GSD})^2 = \frac{\sum C_i (\log D_{p,i} - \log \text{GMD})^2}{\sum C_i}$$

where C_i is the concentration of CP homolog collected on stage i , and $D_{p,i}$ is the geometric mean particle diameter on stage i .

2.5. Respiratory inhalation and deposition modeling

Size distribution data were used to calculate the fractions of particle-bound SCCPs and MCCPs that could be breathed in via the nose and/or mouth (inhalable fraction, IF), enter the lungs gradually below the larynx (thoracic fraction, TF), and are deposited deep into the area for gaseous exchange (respirable fraction, RF) according to the criteria provided by the International Standards Organization and American Conference of Governmental Industrial Hygienists (Hinds, 1999; Luo et al., 2014a, 2016;). In order to further estimate the deposition efficiency (DE) and deposition flux (F) of particle-bound SCCPs and MCCPs in the respiratory tract and its three main regions including head airways region (HA), tracheobronchial region (TB), and alveolar region (AR), a developed model from the International Commission on Radiological Protection (ICRP) was employed (Huang et al., 2016; ICRP, 1994; Yang et al., 2014). More details on the calculation methods can be found in the SI.

3. Results and discussion

3.1. Concentrations and homolog profiles of CPs in indoor airborne PM

Statistical results on the concentrations of SCCPs, MCCPs, and their individual homologs (mean, median, range, and the 5th and 95th percentiles) in indoor airborne PM collected in 10 office rooms and 5 residential houses are summarized in Table 1. More detailed concentration data for each sampling site are listed in Table S1. SCCP and MCCP homologs could be detected in all collected PM samples. The Σ SCCPs and Σ MCCPs in PM ranged from 6.20 to 17.8 ng m^{-3} with a mean of 13.8 ng m^{-3} and from 5.98 to 40.5 ng m^{-3} with a mean of 19.7 ng m^{-3} , respectively. Generally, MCCPs exhibited higher levels than SCCPs in both office and home air PM based on statistical analysis using the t -test ($p < 0.05$). With the phasing out of SCCPs and gradual replacement by

MCCPs as a preferred alternative (Kobeticova and Cerny, 2018), it can be expected that the presence of MCCPs will further increase in the environment. No significant differences in indoor CP levels as well as their compositions were found between these office and home sites (t -test, $p > 0.05$), indicating similar emission sources of CPs in the two types of indoor environments. Therefore, office and home air PM samples were pooled for the analysis and discussion below.

Only three published investigations have identified SCCPs and MCCPs in indoor air (Friden et al., 2011; Gao et al., 2018; Huang et al., 2017). Generally, the concentrations of CPs vary with different types of indoor air samples, for example, gaseous samples, particulate samples (total suspended particle or size-specific particle), or their combination. Thus, it is difficult to directly compare the levels of SCCPs and MCCPs with those from previous studies. Friden et al. (2011) reported that the sum of CP concentrations (SCCPs and MCCPs) were between < 5 –210 ng m^{-3} (mean and median: 69 and 65 ng m^{-3}) in indoor air in Stockholm, Sweden, and the air samples combined gaseous phase with particulate phase. The sum of CP concentrations in the present study was found to be in the range of 12.2–58.3 ng m^{-3} (mean and median: 32.5 and 30.6 ng m^{-3}), slightly lower than the levels in Friden et al.'s study (Friden et al., 2011). In indoor air in Beijing, China, Gao et al. (2018) reported the SCCP concentrations of 9.77–966 ng m^{-3} (mean and median: 181 and 71.9 ng m^{-3}) and MCCP concentrations of < 0.13 –613 ng m^{-3} (mean and median: 41.9 and 3.47 ng m^{-3}) in the gaseous phase, while Huang et al. (2017) reported that the SCCP and MCCP concentrations in the particulate phase of PM_{10} were 38.3–87.7 (mean: 61.1) and 3.2–9.6 (mean: 6.9) ng m^{-3} , respectively. In both studies conducted in Beijing (Gao et al., 2018; Huang et al., 2017), MCCPs exhibited significantly lower levels than SCCPs, which was different from our present findings. The indoor particle-bound SCCP concentrations in Beijing (Huang et al., 2017) were higher than those in Guangzhou in this study, but not for the MCCP concentrations. It is suggested that there are different indoor/outdoor emission sources between the two cities. Moreover, when comparing the indoor air concentrations of CPs with those in the outdoor environment, the indoor CP levels were generally higher than those in ambient air based on the reported studies to date (Friden et al., 2011; Huang et al., 2017; Thanh et al., 2012), indicating that indoor emission sources exist widely at present. It should be noted that differences in air sampling approaches, analytical methods and quantification procedures may lead to some uncertainty in these comparisons.

SCCP and MCCP homolog abundance profiles in the indoor PM samples are illustrated in Fig. S2. C_{10-11} were identified to be the two predominant homolog groups within SCCPs in all samples, accounting for $> 55\%$ of the total composition of SCCPs, followed by C_{13} and C_{12} . The SCCP homolog distribution pattern was roughly similar to that reported in indoor air in Beijing (Gao et al., 2018; Huang et al., 2017), but with a greater proportion of C_{12-13} . A similar homolog profile of MCCPs was observed in all indoor PM samples with C_{14} as the most

Table 1
Concentrations and relative abundance of particle-bound Σ SCCPs and Σ MCCPs and their homolog groups detected in indoor air.

	Concentration (ng m^{-3})					Abundance (%)
	Mean \pm SD	5th percentile	Median	95th percentile	Range	
C10	4.26 \pm 1.32	2.35	4.24	6.30	1.94–7.42	31%
C11	4.35 \pm 1.12	2.63	4.74	5.40	1.96–5.48	31%
C12	2.52 \pm 0.77	1.64	2.08	3.56	1.18–3.62	18%
C13	2.71 \pm 0.86	1.70	2.58	4.19	1.14–4.26	20%
Σ SCCPs	13.8 \pm 3.37	8.55	13.8	17.6	6.20–17.8	100%
C14	9.27 \pm 5.44	3.17	7.94	18.9	3.02–19.7	47%
C15	4.42 \pm 2.50	1.84	3.98	8.96	1.14–9.48	22%
C16	4.08 \pm 1.88	2.20	3.46	7.96	1.30–8.00	21%
C17	1.94 \pm 1.10	0.69	1.64	4.06	0.54–4.16	10%
Σ MCCPs	19.7 \pm 10.7	7.91	16.8	39.6	5.98–40.5	100%

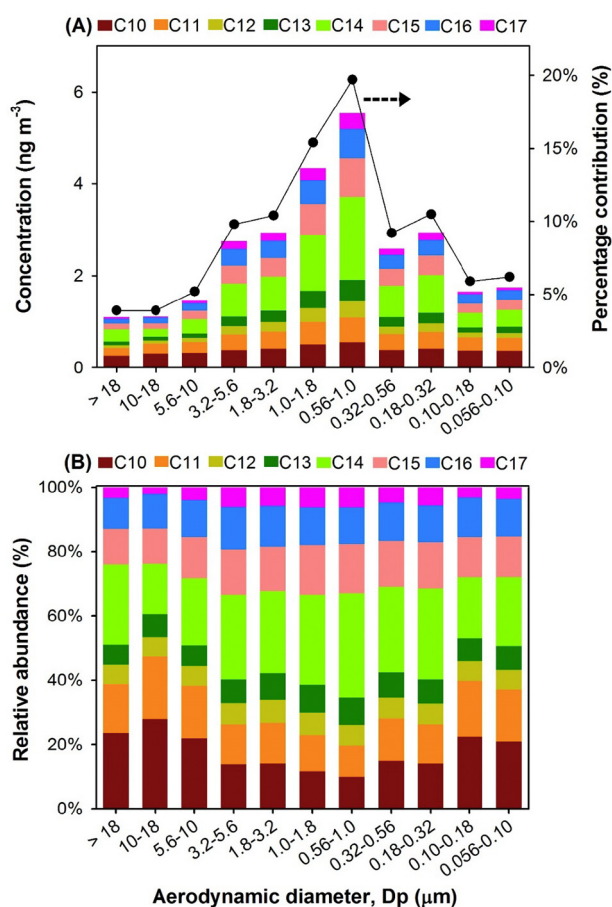


Fig. 1. Size-specific distributions of concentration (A) and relative abundance (B) of CP carbon chain homolog groups (C10–C17) in each size-fractionated particulate matter in indoor air of urban Guangzhou. Fig. (A) also shows the corresponding percentage contributions at each size fraction to the sum concentration (Σ SCCPs + MCCPs).

abundant formula group, which was in agreement with the typical composition profile of MCCPs in commercial mixtures, e.g., CP52. According to chlorine substitution number, Cl_{6–8} groups dominated in both the SCCP and MCCP homolog profiles, corresponding to the chlorine substitution characteristics of commercial CP52 technical mixtures (Gao et al., 2018).

3.2. Size-dependent distribution of CPs in indoor airborne PM and the potential mechanism

Statistical analysis indicated no significant difference in size-dependent distribution of CPs between all sampling sites (*t*-test, $p > 0.05$), so overall mean values as the analytical results are presented and discussed below. The concentration distribution patterns of individual carbon chain homologs and total CPs (SCCPs plus MCCPs, defined as Σ CPs) were determined in size-fractionated PM samples and are illustrated in Fig. 1A. A significant size-dependent distribution of particle-bound CPs can be observed. The size distribution of Σ CPs was obviously categorized by a unimodal peak dominant in 0.56–1.0 μ m fine particles. Overall, the concentration of Σ CPs significantly increased with the decrease of particle size and peaked in fine particles (0.56–1.0 μ m), and then decreased towards more fine and ultrafine particles. The maximum concentration of Σ CPs peaking in the fraction 0.56–1.0 μ m (fine particles) was 5.54 ng m^{-3} . The minimum concentration was found in coarse particles $> 18 \mu\text{m}$ at 1.10 ng m^{-3} . According to the categorization of particle size, concentrations of Σ CPs in the course ($D_p > 1.8 \mu\text{m}$), fine ($0.10 < D_p < 1.8 \mu\text{m}$), and ultrafine

($D_p < 0.10 \mu\text{m}$) particle fractions were 9.34, 17.0, and 1.74 ng m^{-3} , which contributed to 33.1%, 60.6%, and 6.3% of Σ CPs in the total PM, respectively. The results indicate that SCCPs and MCCPs are mainly inclined to adsorb on the fine particle fractions.

Fig. 1B displays the relative abundance of carbon chain homologs (C₁₀–C₁₇) with respect to each size-fractionated PM. An obvious shift to more long-chain CP homologs from the coarse to fine particle fractions was observed in this study. With the decrease of particle size, the relative abundance of longer-chain MCCPs (C_{14–17}) significantly increased and reached a maximum percentage contribution of 65% in the fraction 0.56–1.0 μ m. It can be concluded that the higher concentration distribution of longer-chain MCCPs in the fine particle fractions was mainly attributed to MCCPs being more inclined to adsorb on these midsize fractions. The size-specific distribution of CP homologs with increasing carbon chain length may depend on their physicochemical properties and particle sizes, and the mechanism is further discussed below. In addition, Fig. S3 presents the concentration distribution pattern and relative abundance of chlorine-classified homologs (Cl₅–Cl₁₀) for SCCPs and MCCPs in each size-fraction PM. SCCPs and MCCPs exhibited a similar unimodal distribution with a peak at 0.56–1.0 μ m. For SCCPs, a shift to more heavily chlorinated homologs (Cl₈–Cl₁₀) in the fine particle fractions can be observed, but with no significant changes for MCCPs. This may be due to the variation of physicochemical properties of CP homologs with different chlorine-substituted numbers.

Up to now, no systematic research on the size-dependent distribution of particulate CPs has been reported in indoor air. However, the size distributions of other particle-bound organic contaminants, e.g., persistent organic pollutants (POPs), organophosphate flame retardants (OPFRs), and polycyclic aromatic hydrocarbons (PAHs), in various fractions of PM have been reported (Chrysikou et al., 2009; Hien et al., 2007; Luo et al., 2014b; Luo et al., 2015; Luo et al., 2016; Ni and Zeng, 2013; Yang et al., 2014; Zhang et al., 2012). Similar to the current study, PAHs and polychlorinated biphenyls (PCBs) are inclined to adsorb on fine particles (Chrysikou et al., 2009; Hien et al., 2007). By contrast, brominated flame retardants such as tetrabromobisphenol A (TBBPA) tend to affiliate with coarse particles (Ni and Zeng, 2013). Depending on the molecular structures and volatilities, polybrominated diphenyl ether (PBDE) congeners and OPFR analogs can accumulate predominantly in fine or coarse particles (Luo et al., 2014b; Yang et al., 2014). The conclusion that can be drawn from these studies is that the distribution of pollutants in PM generally depends on the particle size, but the distribution patterns are controlled by both chemical structures and particle sizes.

Furthermore, the particle size distributions ($dC/C \text{ dlog } D_p$ versus D_p) of individual carbon chain homologs (C₁₀–C₁₇), Σ SCCPs (C₁₀–C₁₃), and Σ MCCPs (C₁₄–C₁₇) in the collected PM in indoor air are shown in Fig. 2. It is evident that individual carbon chain homologs, Σ SCCPs and Σ MCCPs shared a similar unimodal distribution pattern peaking in the fraction 0.56–1.0 μ m, and longer chain homologs were inclined to shift from coarse particles to fine particles. As shown in Fig. 3A, the mass fractions in fine particles (MFFP, $D_p < 1.8 \mu\text{m}$) increased significantly with increasing carbon atom number for SCCPs ($p < 0.01$), but not for MCCPs. The size distributions of individual chlorine-classified homologs (Cl₅–Cl₁₀) are presented in Fig. S4. It was found that Cl₅–Cl₉ also exhibited a similar unimodal distribution characterized by a peak at 0.56–1.0 μ m, but Cl₁₀ shared a bimodal distribution pattern with two peaks at 0.56–1.0 and 3.2–5.6 μ m, respectively. A significant increase in the MFFP with increasing chlorine atom number/chlorine content was found for SCCPs ($p < 0.05$) (Fig. S4A), but not for MCCPs (Fig. S4B).

To explore the potential mechanism behind the size distribution of CPs, the GMD and GSD were calculated and the related statistical analysis was conducted. As shown in Fig. 3B, the mean GMD values for C₁₀–C₁₇ homologs varied from 1.00 to 1.36 μm , which is in the range of fine particle diameter. The GMD values were found to decrease significantly with an increase of carbon chain length of SCCPs ($p < 0.05$).

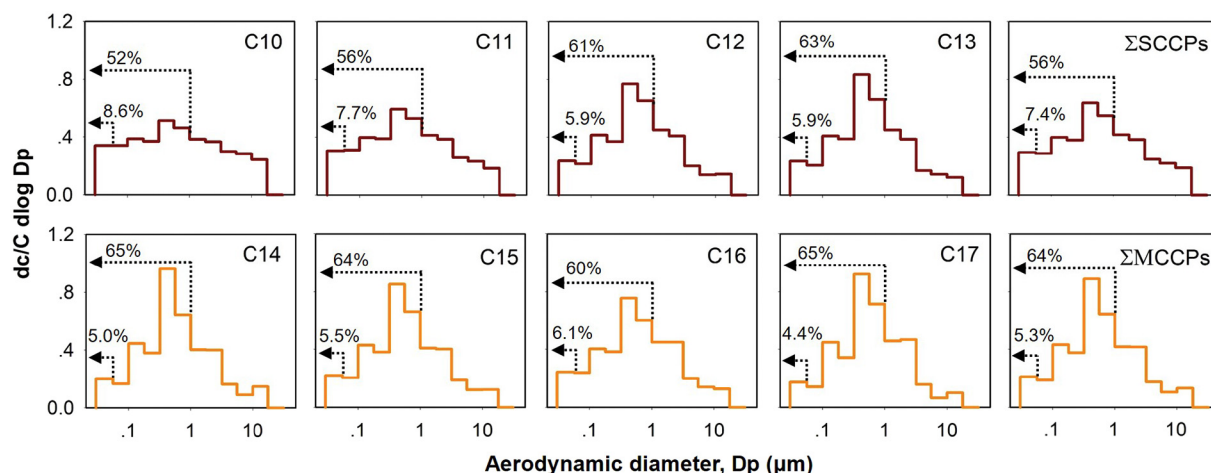


Fig. 2. Size-dependent distributions of particle-bound SCCPs, MCCPs and individual carbon chain homolog groups (C10–C17) in indoor air of urban Guangzhou. dc is the concentration on each filter, C is the sum concentration on all filters and $d \log D_p$ is the logarithmic size interval for each impactor stage in aerodynamic diameter (D_p). Dotted arrows at 0.10 and 1.8 μm show ultrafine and fine mode, respectively, and the corresponding values (%) show the corresponding percentage contributions to the sum concentration.

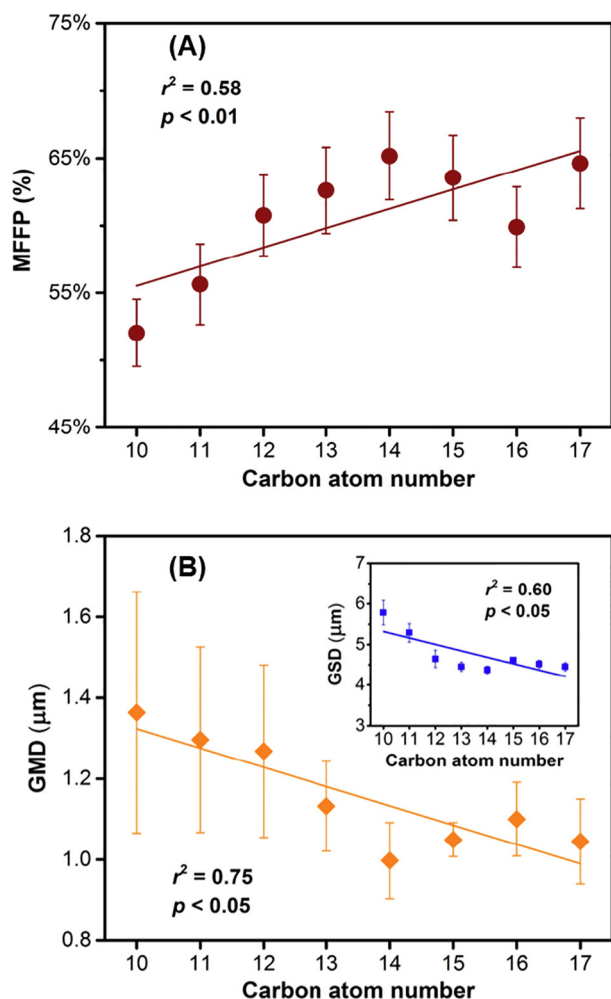


Fig. 3. (A) A significant correlation between mass fractions in fine particles (MFPP, fine particle: aerodynamic diameter < 1.8 μm) and carbon atom number of CP homologs; (B) A significant correlation between geometric mean diameter (GMD) or geometric standard deviation (GSD) and carbon atom number of the CP homolog.

Moreover, the GSD values also decreased significantly with an increase of carbon chain length of SCCPs ($p < 0.05$), suggesting a broader size distribution for shorter-chain homologs. The distribution of CP homologs in particles of different size may be associated with their physicochemical properties. Previous studies indicated that vapor pressure (V_p) is a key factor governing the particle size distribution of some organic pollutants, e.g., PAHs (Zhang et al., 2012), PBDEs (Luo et al., 2014b), and OPFRs (Yang et al., 2014). Due to a lack of V_p data for CP homologs to date, further correlation analysis between the GMD/GSD and V_p was not conducted. However, Drouillard et al. (1998) reported a decline in vapor pressures of CP homologs (C₁₀–C₁₂) with increasing carbon chain length and chlorine content. The carbon chain length and chlorine content are directly related to CP molecular weight (MW), which is a key property controlling the vapor pressure of CP homologs. Based on the conclusion by Drouillard et al. (1998), we infer that the V_p for SCCPs (C₁₀–C₁₃) with lower MW can be easily and monotonically affected by carbon chain length or chlorine substitution number, but for MCCPs (C₁₄–C₁₇) with higher MW, their V_p may neither be monotonically affected by carbon atom number nor chlorine substitution number. This provides a possible explanation for the significant correlations between MFPP/GMD and carbon chain length for SCCPs, but not for MCCPs. Based on the key findings and correlation analysis above, we can conclude that longer-chain and higher chlorinated CP homologs with higher MW and lower V_p can easily adsorb onto small particles with large surface areas due to the increasing hydrophobicity, whereas shorter-chain and lower chlorinated CP homologs with lower MW and higher V_p may more easily migrate to coarse particles from fine particles through volatilization and condensation processes. The determination of V_p for CPs and the proposed mechanism related to V_p and MW for the size-dependent distribution of CPs merit adequate investigations in the near future.

3.3. Regional deposition of SCCPs and MCCPs in the human respiratory tract

Thus far, only a couple of studies have reported on indoor exposure assessment of CPs using the U.S. EPA model (Friden et al., 2011), and only estimated the whole inhalation of gaseous and/or particulate CPs, but they did not consider particulate CP deposition in the respiratory tract. In fact, only parts of the inhalable particulate pollutants can accumulate in the respiratory tract. In addition, different sized particles have different efficiencies of size-specific deposition in the respiratory system, which will directly result in their different contributions to

Table 2

The inhalable fraction (IF, %), thoracic fraction (TF, %) and respirable fraction (RF, %) of particle-bound SCCPs and MCCPs in the human respiratory tract, and deposition efficiency (DE, %) and deposition flux (F, pg h^{-1}) of particle-bound SCCPs and MCCPs in the human respiratory tract and its three main regions, i.e., the head region (HR), tracheobronchial region (TR), and alveolar region (AR).

	Inhalable fraction (%)	Thoracic fraction (%)	Respirable fraction (%)	Deposition efficiency (%)				Deposition flux (pg h^{-1})			
				HR	TR	AR	Total	HR	TR	AR	Total
C10	90.9	81.6	68.4	40.1	2.56	8.30	51.0	1130	72.1	233	1440
C11	91.1	82.3	69.1	40.7	2.61	8.34	51.6	1170	75.4	240	1490
C12	91.4	83.2	70.1	41.3	2.64	8.30	52.3	686	44.2	138	868
C13	92.2	85.2	73.2	39.3	2.64	8.53	50.5	702	47.6	154	903
Σ SCCPs	91.3	82.8	69.8	40.4	2.61	8.35	51.4	3690	239	765	4690
C14	93.0	87.2	76.2	36.7	2.50	8.53	47.8	2180	152	529	2860
C15	93.2	87.6	76.7	35.6	2.49	8.63	46.7	1010	71.9	253	1330
C16	92.6	86.4	74.7	37.5	2.55	8.53	48.6	995	69.0	232	1300
C17	92.8	87.0	75.6	37.9	2.57	8.51	49.0	480	33.3	110	623
Σ MCCPs	92.9	87.1	75.9	36.8	2.52	8.56	47.9	4660	326	1120	6110
Σ SCCPs + MCCPs	92.3	85.3	73.3	38.3	2.56	8.47	49.3	8350	566	1890	10,800

deposition regions of the respiratory tract based on the size-specific distribution. In order to further understand the significance of size dependency in the inhalation exposure assessment of particle-bound CPs, the inspirable, thoracic and respirable fractions of CPs according to the principles defined by the International Standards Organization and American Conference of Governmental Industrial Hygienists were estimated (Hinds, 1999). Furthermore, the deposition efficiencies and deposition fluxes of CPs based on the ICRP model (IPCS, 1996) were also calculated using the size-dependent data acquired in this study. As shown in Table 2, the estimated inspirable, thoracic and respirable fractions of CPs were 90.9–93.2%, 81.6–87.6%, and 68.4–76.7%, respectively. In comparison, only 46.7–52.3% of CPs could ultimately accumulate in the respiratory tract as defined by the ICRP model. This result is comparable to those for PBDEs (Luo et al., 2014a). Apparently, not all inhalable particle-bound CPs can deposit in the human respiratory system.

The total flux of depositions and their efficiencies were 4.69 ng h^{-1} and 51.4% for Σ SCCPs and 6.11 ng h^{-1} and 47.9% for Σ MCCPs in the entire respiratory tract respectively. The deposition fluxes and efficiencies of individual CP homologs (C₁₀–C₁₇) were 0.48 – 2.18 ng h^{-1} and 35.5–42.3% in the head airways, 0.033 – 0.15 ng h^{-1} and 2.49–2.64% in the tracheobronchial region, and 0.11 – 0.53 ng h^{-1} and 8.30–8.53% in the alveolar region (Table 2). The results indicate that the majority of inhalable particle-bound CPs deposited in the head airways, and only a small portion deposited in the lungs. Compared to the alveolar region, deposition in the head airways generally would cause relatively lower health hazards. The deposition fluxes of particle-bound CPs in these three regions of the human respiratory tract were also found to be size-dependent. The relative contributions of size-fractionated CPs deposited in different regions of the respiratory tract are shown in Fig. 4 and S5. Evidently, coarse particles were dominant in the head airway (70.7–81.2%), but fine particles contributed the most in the alveolar region (53.7–67.8%). It is important to note that ultrafine particles contributed 8.8–20.6% of the alveolar deposition. In the tracheobronchial region, the relative contributions of coarse particles and fine particles were almost equal at 49.9–56.4% and 32.5–42.9%, respectively. This finding is similar to a previous study on PBDEs (Luo et al., 2014a). Moreover, it should also be noted that with the increase of carbon chain length or degree of chlorination (Fig. 4 and S5), the relative contributions of coarse and ultrafine particles decreased gradually, but those of fine particles increased correspondingly. The variations of relative contributions of different size-fractionated particles to CP homolog deposition in the three respiratory tract regions were mainly attributed to their size-specific distributions governed by the vapor pressure. Overall, all weights of evidence indicate that particle size distribution is a key factor in dictating human inhalation exposure to particle-bound CPs, and should be taken into account for human

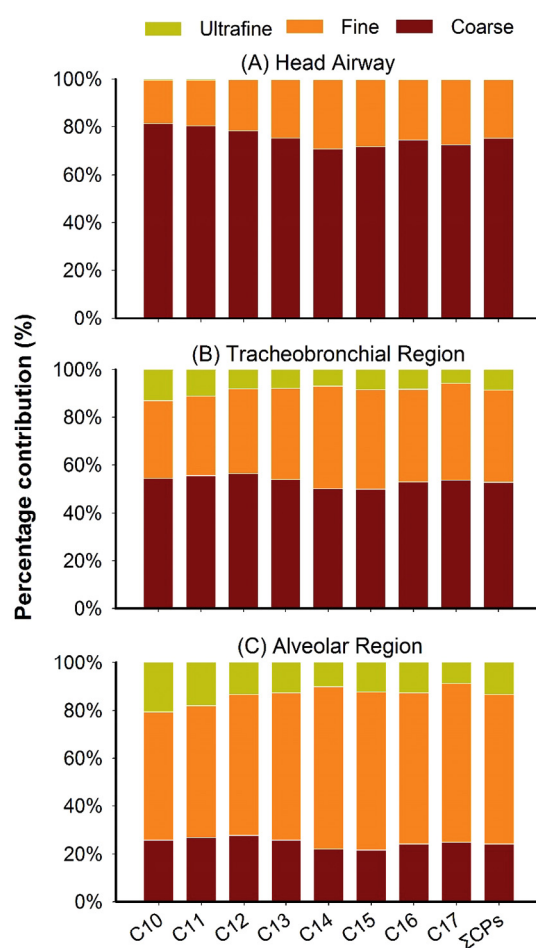


Fig. 4. Relative contributions of coarse, fine, and ultrafine particles in indoor air of urban Guangzhou to the deposition fluxes of individual carbon chain homolog groups (C₁₀–C₁₇), and total SCCPs and MCCPs (defined as Σ CPs) in the (A) head, (B) tracheobronchial, and (C) alveolar regions of the human respiratory tract.

health risk assessment. This is the first report on the size-dependent distribution of regional deposition of particulate CPs in the human respiratory tract.

Table 3
Exposure assessments of SCCPs and MCCPs via inhalation of particulate matter in indoor air^a.

Compounds	TDI values ^b	CP inhalation based on EPA model ^c			CP inhalation based on ICRP model ^d		
		5th percentile	Median	95th percentile	5th percentile	Median	95th percentile
ΣSCCPs	100,000	1.81	2.92	3.72	0.91	1.60	1.91
ΣMCCPs	100,000	1.67	3.56	8.38	0.86	1.74	4.22
ΣSCCPs + MCCPs	–	3.48	6.48	12.1	1.78	3.34	6.12

^a Unit is ng kg⁻¹ day⁻¹.

^b Values are from the references (De Boer et al., 2010; IPCS, 1996).

^c Inhalation rate is 16 m³ day⁻¹ for a 31–51 year old adult. The body weight of an adult is set as 63 kg. The estimated residence time for an adult in indoor environment is 20 h day⁻¹.

^d Data are calculated from the parameters in Table 2.

3.4. Potential health risk from exposure to indoor size-fractionated SCCPs and MCCPs

SCCPs and MCCPs can go into the human body via various external exposure routes, among which inhalation of particulate matter is believed to be the main route for indoor exposure to CPs. Exposure assessments of SCCPs and MCCPs via inhalation of PM in indoor air were performed according to the exposure levels determined by the U.S. EPA model and based on the deposition fluxes by the ICRP model, respectively. We compared the two models for inhalation exposure assessments under low, median, and high exposure scenarios (Table 3). Inhalation exposure doses of SCCPs and MCCPs calculated by the U.S. EPA model were 2.92 and 3.56 ng kg⁻¹ day⁻¹, approximately two times higher than those derived from the ICRP model. This was due to the fact that the ICRP model took into account the deposition efficiencies of size-fractionated CPs in the human respiratory tract. Overall, the estimated inhalation exposure levels of SCCPs, MCCPs, or even their sum were much lower than the recommended tolerable daily intake (TDI) values (100 μg kg⁻¹ day⁻¹) suggested by the International Programme on Chemical Safety (De Boer et al., 2010; IPCS, 1996). This indicates no significant exposure risk of SCCPs and MCCPs for human health via indoor PM inhalation at present.

However, it should be noted that inhalation exposure to particulate CPs can only take up part of the exposure risk to air CPs, particularly for shorter-chain and lower chlorinated homologs with relatively high volatility. Thus, gaseous CPs in indoor environment deserves further investigation to elucidate the overall risk due to exposure to atmospheric CPs. In addition, it is still difficult to accurately assess the health risk in indoor environments due to lack of official threshold values for CP exposure in regard to human health. Comprehensive assessment for indoor exposure to CPs is therefore urgently needed.

4. Conclusions

This study has demonstrated the current levels and homolog profiles of CPs in indoor air PM in typical urban indoor environments. The size-dependent distributions of particle-bound SCCPs and MCCPs in indoor air were characterized by a unimodal distribution pattern peaking in the fine particle fraction 0.56–1.0 μm. Longer-chain homologs tend to shift from coarse particles to fine particles during the partitioning. Vapor pressure may be a critical factor governing the particle size distribution of CPs. Deposition of particle-bound CPs in different respiratory tract regions is also size-dependent. Coarse particles contributed the most in the head airway, while fine particles were dominant in the alveolar region. Moreover, the relative contributions of fine particles to the regional deposition of CPs in the human respiratory tract increased with increase of carbon chain length or chlorine content. Taking into account the size-dependent distribution of CPs, inhalation exposure assessment based on the ICRP model indicates a low risk of inhalation exposure to CPs in the general indoor environments in China.

Acknowledgements

This work was financially supported by the National Natural Science Foundation of China (Nos. 41522304, 21577142, and 21876063), Guangdong (China) Innovative and Entrepreneurial Research Team Program (2016ZT06N258), and the Fundamental Research Funds for the Central Universities.

Appendix A. Supplementary data

Supplementary data to this article can be found online at <https://doi.org/10.1016/j.envint.2018.10.004>.

References

- Chrysikou, L.P., Gemenetzi, P.G., Samara, C.A., 2009. Wintertime size distribution of polycyclic aromatic hydrocarbons (PAHs), polychlorinated biphenyls (PCBs) and organochlorine pesticides (OCPs) in the urban environment: street- vs rooftop-level measurements. *Atmos. Environ.* 43, 290–300.
- De Boer, J., El-Sayed Ali, T., Fiedler, H., Legler, J., Muir, D.C., Nikiforov, V.A., Tomy, G.T., Tsunemi, K., 2010. Chlorinated paraffins. In: *The Handbook of Environmental Chemistry*. 10. Springer, Berlin Heidelberg, Germany, pp. 1–40.
- Drouillard, K.G., Tomy, G.T., Muir, D.C.G., Friesen, K.J., 1998. Volatility of chlorinated n-alkanes (C₁₀–C₁₂): vapor pressures and Henry's law constants. *Environ. Toxicol. Chem.* 17, 1252–1260.
- Friden, U.E., McLachlan, M.S., Berger, U., 2011. Chlorinated paraffins in indoor air and dust: concentrations, congener patterns, and human exposure. *Environ. Int.* 37, 1169–1174.
- Gallistl, C., Sprengel, J., Vetter, W., 2018. High levels of medium-chain chlorinated paraffins and polybrominated diphenyl ethers on the inside of several household baking oven doors. *Sci. Total Environ.* 615, 1019–1027.
- Gao, W., Cao, D., Wang, Y., Wu, J., Wang, Y., Wang, Y.W., Jiang, G.B., 2018. External exposure to short- and medium-chain chlorinated paraffins for the general population in Beijing, China. *Environ. Sci. Technol.* 52, 32–39.
- Glüge, J., Wang, Z., Bogdal, C., Scheringer, M., Hungerbuehler, K., 2016. Global production, use, and emission volumes of short-chain chlorinated paraffins - a minimum scenario. *Sci. Total Environ.* 573, 1132–1146.
- Glüge, J., Schinkel, L., Hungerbuehler, K., Cariou, R., Bogdal, C., 2018. Environmental risks of medium-chain chlorinated paraffins (MCCPs) - a review. *Environ. Sci. Technol.* 52, 6743–6760.
- Hien, T.T., Thanh, L.T., Kameda, T., Takenaka, N., Bandow, H., 2007. Distribution characteristics of polycyclic aromatic hydrocarbons with particle size in urban aerosols at the roadside in Ho Chi Minh City, Vietnam. *Atmos. Environ.* 41, 1575–1586.
- Hilger, B., Fromme, H., Völkel, W., Coelhan, M., 2013. Occurrence of chlorinated paraffins in house dust samples from Bavaria, Germany. *Environ. Pollut.* 175, 16–21.
- Hinds, W.C., 1999. *Aerosol Technology: Properties, Behavior, and Measurement of Airborne Particles*, 2nd ed. Wiley Interscience, New York.
- Huang, C.L., Bao, L.J., Luo, P., Wang, Z.Y., Li, S.M., Zeng, E.Y., 2016. Potential health risk for residents around a typical e-waste recycling zone via inhalation of size-fractionated particle-bound heavy metals. *J. Hazard. Mater.* 317, 449–456.
- Huang, H.T., Gao, L.R., Xia, D., Qiao, L., Wang, R.H., Su, G.J., Liu, W.B., Liu, G.R., Zheng, M.H., 2017. Characterization of short- and medium-chain chlorinated paraffins in outdoor/indoor PM₁₀/PM_{2.5}/PM_{1.0} in Beijing, China. *Environ. Pollut.* 225, 674–680.
- ICRP, 1994. Publication 66: human respiratory tract model for radiological protection. *Ann. ICRP* 24, 1–3.
- IPCS, 1996. Environmental Health Criteria 181: Chlorinated Paraffins. International Programme on Chemical Safety, Geneva, Switzerland. <http://www.inchem.org/documents/ehc/ehc/ehc181.htm>, Accessed date: January 2018.
- Kobeticova, K., Cerny, R., 2018. Ecotoxicity assessment of short- and medium-chain chlorinated paraffins used in polyvinyl-chloride products for construction industry.

- Sci. Total Environ. 640–641, 523–528.
- Lao, J.Y., Wu, C.C., Bao, L.J., Liu, L.Y., Shi, L., Zeng, E.Y., 2018. Size distribution and clothing-air partitioning of polycyclic aromatic hydrocarbons generated by barbecue. *Sci. Total Environ.* 639, 1283–1289.
- Li, C., Xie, H.B., Chen, J., Yang, X., Zhang, Y., Qiao, X., 2014. Predicting gaseous reaction rates of short chain chlorinated paraffins with center dot OH: overcoming the difficulty in experimental determination. *Environ. Sci. Technol.* 48, 13808–13816.
- Luo, P., Bao, L.J., Wu, F.C., Li, S.M., Zeng, E.Y., 2014a. Health risk characterization for resident inhalation exposure to particle-bound halogenated flame retardants in a typical e-waste recycling zone. *Environ. Sci. Technol.* 48, 8815–8822.
- Luo, P., Ni, H.G., Bao, L.J., Li, S.M., Zeng, E.Y., 2014b. Size distribution of airborne particle-bound polybrominated diphenyl ethers and its implications for dry and wet deposition. *Environ. Sci. Technol.* 48, 13793–13799.
- Luo, P., Bao, L.J., Li, S.M., Zeng, E.Y., 2015. Size-dependent distribution and inhalation cancer risk of particle-bound polycyclic aromatic hydrocarbons at a typical e-waste recycling and an urban site. *Environ. Pollut.* 200, 10–15.
- Luo, P., Bao, L.J., Guo, Y., Li, S.M., Zeng, E.Y., 2016. Size-dependent atmospheric deposition and inhalation exposure of particle-bound organophosphate flame retardants. *J. Hazard. Mater.* 301, 504–511.
- Ni, H.G., Zeng, H., 2013. HBCD and TBPPA in particulate phase of indoor air in Shenzhen, China. *Sci. Total Environ.* 458, 15–19.
- Thanh, W., Han, S., Yuan, B., Zeng, L.X., Li, Y., Wang, Y.W., Jiang, G.B., 2012. Summer-winter concentrations and gas-particle partitioning of short chain chlorinated paraffins in the atmosphere of an urban setting. *Environ. Pollut.* 171, 38–45.
- UNEP, 2016. Report of the Persistent Organic Pollutants Review Committee on the Work of its Twelfth Meeting: Risk Management Evaluation on Short-chain Chlorinated Paraffins (UNEP/POPS/POPRC.12/11/Add.3).
- UNEP, 2017. Recommendation by the Persistent Organic Pollutants Review Committee to List Short-chain Chlorinated Paraffins in Annex A to the Convention and Draft Text of the Proposed Amendment (UNEP/POPS/COP.8/14).
- van Mourik, L.M., Gaus, G., Leonards, P.E.G., De Boer, J., 2016. Chlorinated paraffins in the environment a review on their production, fate, levels and trends between 2010 and 2015. *Chemosphere* 155, 415–428.
- Wang, Y.W., Gao, W., Jiang, G.B., 2017. Strengthening the study on the behavior and transformation of medium-chain chlorinated paraffins in the environment. *Environ. Sci. Technol.* 51, 10282–10283.
- Xu, C., Xu, J.H., Zhang, J.B., 2014. Emission inventory prediction of short chain chlorinated paraffins (SCCPs) in China. *Acta Sci. Nat. Univ. Pekin.* 50, 369–378.
- Yang, F., Ding, J., Huang, W., Xie, W., Liu, W., 2014. Particle size-specific distributions and preliminary exposure assessments of organophosphate flame retardants in office air particulate matter. *Environ. Sci. Technol.* 48, 63–70.
- Zeng, L.X., Wang, T., Han, W.Y., Yuan, B., Liu, Q.A., Wang, Y.W., Jiang, G.B., 2011. Spatial and vertical distribution of short chain chlorinated paraffins in soils from wastewater irrigated farmlands. *Environ. Sci. Technol.* 45, 2100–2106.
- Zeng, L.X., Zhao, Z.S., Li, H.J., Han, W.Y., Liu, Q., Xiao, K., Du, Y.G., Wang, Y.W., Jiang, G.B., 2012. Distribution of short chain chlorinated paraffins in marine sediments of the East China Sea: influencing factors, transport and implications. *Environ. Sci. Technol.* 46, 9898–9906.
- Zeng, L.X., Chen, R., Zhao, Z.S., Wang, T., Gao, Y., Li, A., Wang, Y.W., Jiang, G.B., Sun, L.G., 2013. Spatial distributions and deposition chronology of short chain chlorinated paraffins in marine sediments across the Chinese Bohai and yellow seas. *Environ. Sci. Technol.* 47, 11449–11456.
- Zeng, L.X., Lam, J.C.W., Wang, Y.W., Jiang, G.B., Lam, P.K.S., 2015. Temporal trends and pattern changes of short- and medium-chain chlorinated paraffins in marine mammals from the South China Sea over the past decade. *Environ. Sci. Technol.* 49, 11348–11355.
- Zeng, L.X., Lam, J.C.W., Chen, H., Du, B.B., Leung, K.M.Y., Lam, P.K.S., 2017a. Tracking dietary sources of short- and medium-chain chlorinated paraffins in marine mammals through a subtropical marine food web. *Environ. Sci. Technol.* 51, 9543–9552.
- Zeng, L.X., Lam, J.C.W., Horii, Y., Li, X.L., Chen, W.F., Qiu, J.W., Leung, K.M.Y., Yamazaki, E., Yamashita, N., Lam, P.K.S., 2017b. Spatial and temporal trends of short- and medium-chain chlorinated paraffins in sediments off the urbanized coastal zones in China and Japan: a comparison study. *Environ. Pollut.* 224, 357–367.
- Zhan, F., Zhang, H., Wang, J., Xu, J., Yuan, H., Gao, Y., Su, F., Chen, J., 2017. Release and gas-particle partitioning behaviors of short-chain chlorinated paraffins (SCCPs) during the thermal treatment of polyvinyl chloride flooring. *Environ. Sci. Technol.* 51, 9005–9012.
- Zhang, K., Zhang, B.Z., Li, S.M., Wong, C.S., Zeng, E.Y., 2012. Calculated respiratory exposure to indoor size-fractionated polycyclic aromatic hydrocarbons in an urban environment. *Sci. Total Environ.* 431, 245–251.
- Zhu, X., Bai, H., Gao, Y., Chen, J., Yuan, H., Wang, L., Wang, W., Dong, X., Li, X., 2017. Concentrations and inhalation risk assessment of short-chain polychlorinated paraffins in the urban air of Dalian, China. *Environ. Sci. Pollut. R.* 24, 21203–21212.